APPENDIX 1. Correction of Filter-Filter-Denuder Sampling Train Data for Gas-Phase PAH Adsorption on Filters

Two methods for correcting the filter-filter-denuder (FFD) sampling train data to account for adsorption of gas-phase PAHs on the filters were considered: (a) subtracting the mass of a given PAH observed on the backup filter from the particle-phase PAH mass and adding it to the gas-phase PAH mass or (b) performing the same correction, but calculating the fraction of the total gas-phase mass that is adsorbed by the front filter using the observed mass on the backup filter. The first option was used in this study because the results of sampling event "chamber 4" (Table 1) in which four FFD systems were run simultaneously at different flow rates (and thus different sampling volumes) showed similar PAH masses adsorbed on each of the backup filters (data not shown). This suggests that the filter material had reached equilibrium with respect to PAH adsorption over the flow rates and sampling times used in this study. Since the fraction of the filter surface occupied by particles is small on the front filter (calculated as < 1% for all samples in this study), the PAH mass adsorbed on the backup filter should be similar to that adsorbed on the front filter.

Accordingly, the gas- and particle-phase concentrations for each PAH were obtained from the following expressions:

$$C_g(\mathrm{ng/m^3}) = \frac{M_D + 2M_{BF}}{V_{sample}} \qquad \text{(A1-1)}$$

$$C_p(\mathrm{ng/m^3}) = \frac{M_{FF} - M_{BF}}{V_{sample}} \qquad \text{(A1-2)}$$

where M_D, M_{BF}, and M_{FF} are the masses of the PAH collected by the denuder, the backup filter, and the front filter, respectively, and V_{sample} is the volume of the sample. The magnitude of the artifact can be calculated according to the following expressions:

$$E_g = \frac{\text{mass adsorbed on backup filter}}{\text{corrected gas - phase mass}} = \frac{M_{BF}}{M_D + 2M_{BF}} \quad \text{(A1-3)}$$

$$E_p = \frac{\text{mass adsorbed on backup filter}}{\text{corrected particle - phase mass}} = \frac{M_{BF}}{M_{FF} - M_{BF}} \quad \text{(A1-4)}$$

where E_g and E_p are the errors in the measured gas- and particle-phase PAH concentrations, respectively, that would have been obtained if a backup filter had not been used and the data had not been corrected. Results for the deuterated PAHs used in this study are shown in Figures A1-1 and A1-2. Note that these artifacts are significant, especially the E_g values for the larger PAHs (e.g., benz(a)anthracene-d_{12}) and the E_p values for the smaller PAHs (e.g., fluorene-d_{10}). This is because the gas-phase PAH concentration is lower for the larger PAHs. As such, the gas-phase mass adsorbed on the filter constitutes a significant fraction of the total gas-phase mass for the compound. Alternately, the smaller PAHs partition more to the gas phase and less to the particle phase. As such, the gas-phase mass adsorbed on the filter constitutes a significant fraction of the total particle-phase mass for the compound.

It was assumed that desorption of PAHs from the particles on the front filter in the FFD system was insignificant for chamber samples. This is because: (a) the pressure drop across the

filter was low (12.3 to 14.6 Torr), (b) the sampled gas-phase concentration does not change significantly over the course of a sampling event, and (c) the results of sample "chamber 4" (Table 1) showed that the measured gas- and particle-phase concentrations did not change significantly at different sampling face velocities ranging from 21 to 44 cm/sec. The assumption of insignificant desorption is also corroborated by studies showing that the artifact resulting from desorption from particles collected on the filters is much smaller than the artifact resulting from the adsorption of gas-phase analytes on the filter material for this type of sample (*22*, *23*).

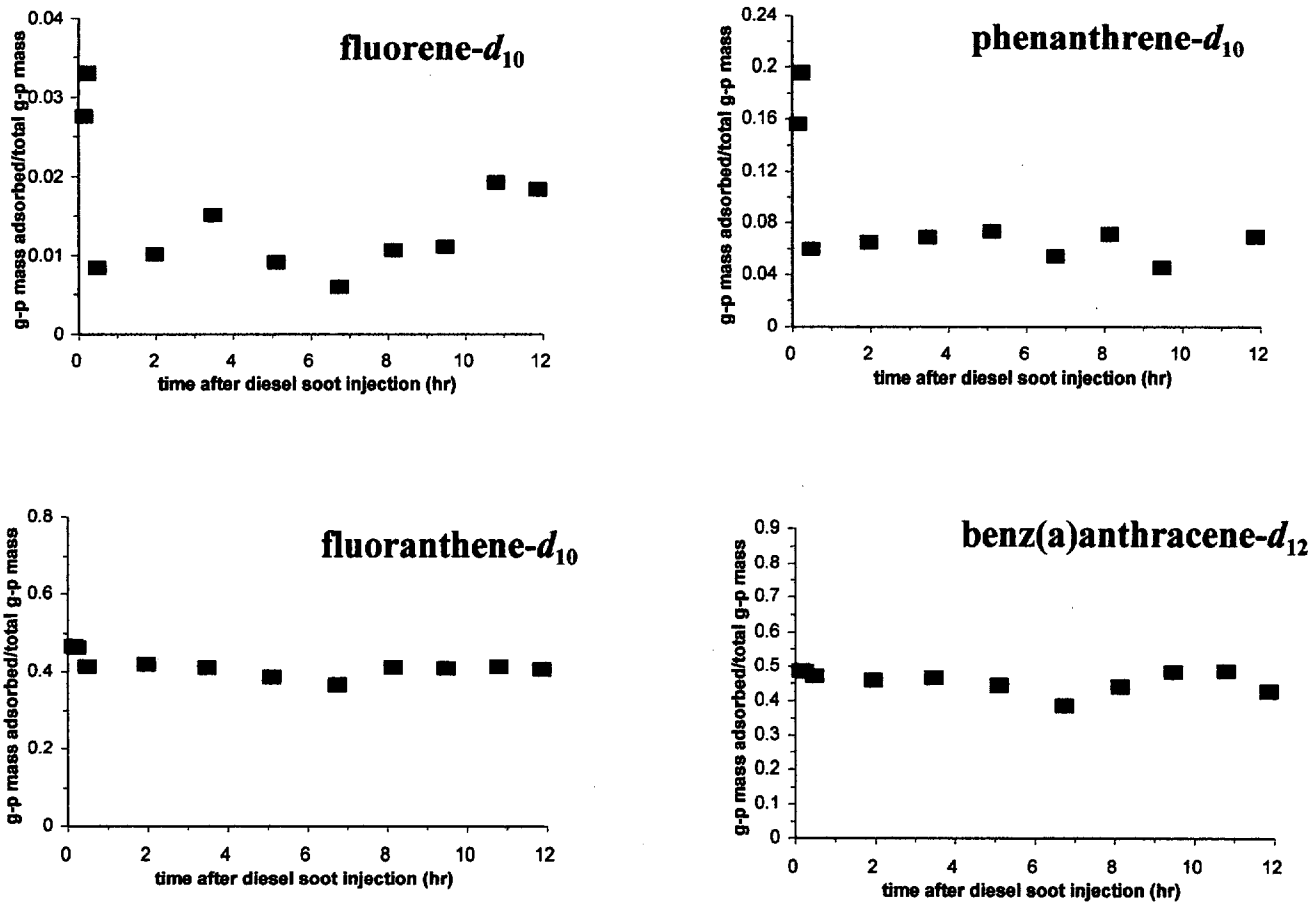

FIGURE A1-1. Experimental E_g results; the error in the measured gas-phase PAH concentration that would have been obtained if a backup filter had not been used and the data had not been corrected (see eq A1-3).

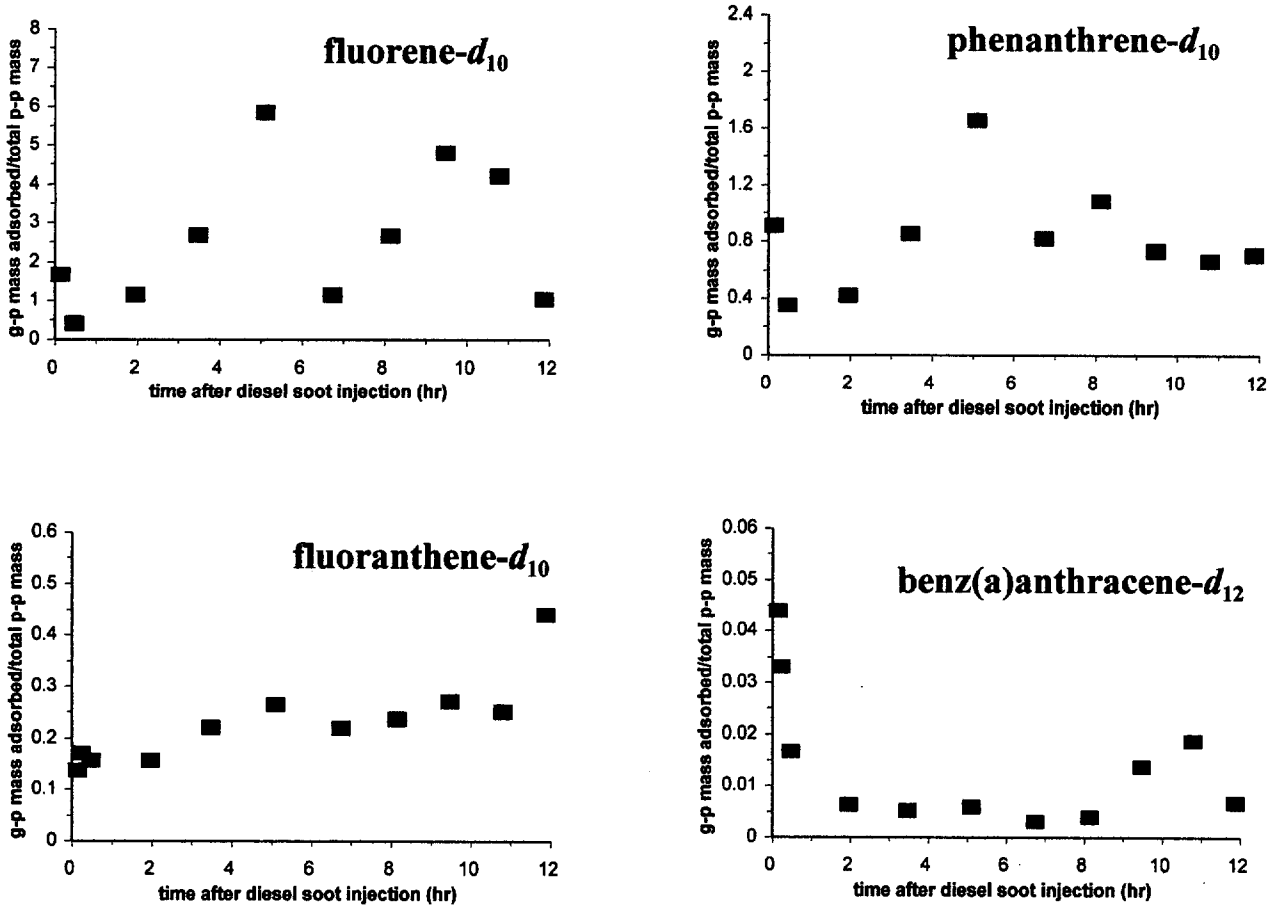

FIGURE A1-2. Experimental E_p results; the error in the measured particle-phase PAH concentration that would have been obtained if a backup filter had not been used and the data had not been corrected (see eq A1-4).

APPENDIX 2. Determination of K_p Values

Equilibrium K_p values were obtained using the following semi-empirical relationship (*19*, *46*):

$$\log K_p = a_{emp} \log p_L^\circ + c_{emp} \qquad \text{(A2-1)}$$

where p_L° is the pure compound liquid vapor pressure (subcooled if necessary), and a_{emp} and c_{emp} are empirical constants for each compound. The value of a_{emp} for each deuterated PAH used in this study was obtained using a database of equilibrium K_p vs temperature (and thus p_L°) data compiled from diesel soot smog chamber experiments conducted by our group over the past four years as discussed by Strommen and Kamens (*19*). c_{emp} values for each compound could have been obtained from the same database. However, in order to obtain more accurate equilibrium K_p estimates by reducing inter-experiment variability not captured in the regression of the database values, the c_{emp} value for each compound was obtained from measurements of the non-deuterated (i.e., native) PAHs from the first chamber sample in the present study. A plot of the logarithm of the observed K_p values vs $\log p_L^\circ$ for the non-deuterated PAHs in this sample was linear (r^2=0.98) with a slope near -1 (slope = -1.09). As demonstrated by Pankow (*28*), this indicates that the non-deuterated PAHs were near gas-particle equilibrium. Accordingly, the value of c_{emp} for each deuterated PAH was obtained using eq A2-1 and: (a) the observed (i.e., equilibrium) K_p value for the non-deuterated analogue of the deuterated PAH of interest and (b) the deuterated PAH's database a_{emp} value discussed above. p_L° values (as a function of temperature) for non-deuterated PAHs were obtained from Yamasaki (*47*). The p_L° values for the deuterated PAHs were obtained by implementing the gas-chromatographic relative retention time technique of Hamilton (*48*, *49*) using the non-deuterated PAH analogues as reference compounds (e.g., fluoranthene was used as a reference compound for fluoranthene-d_{10}).

© 1999 American Chemical Society, Environ. Sci. Technol., Strommen es981035q Supporting Info Page 7

APPENDIX 3. Experimental vs Simulation Results for Fluorene-d_{10}, Phenanthrene-d_{10}, and Benz(a)anthracene-d_{12}

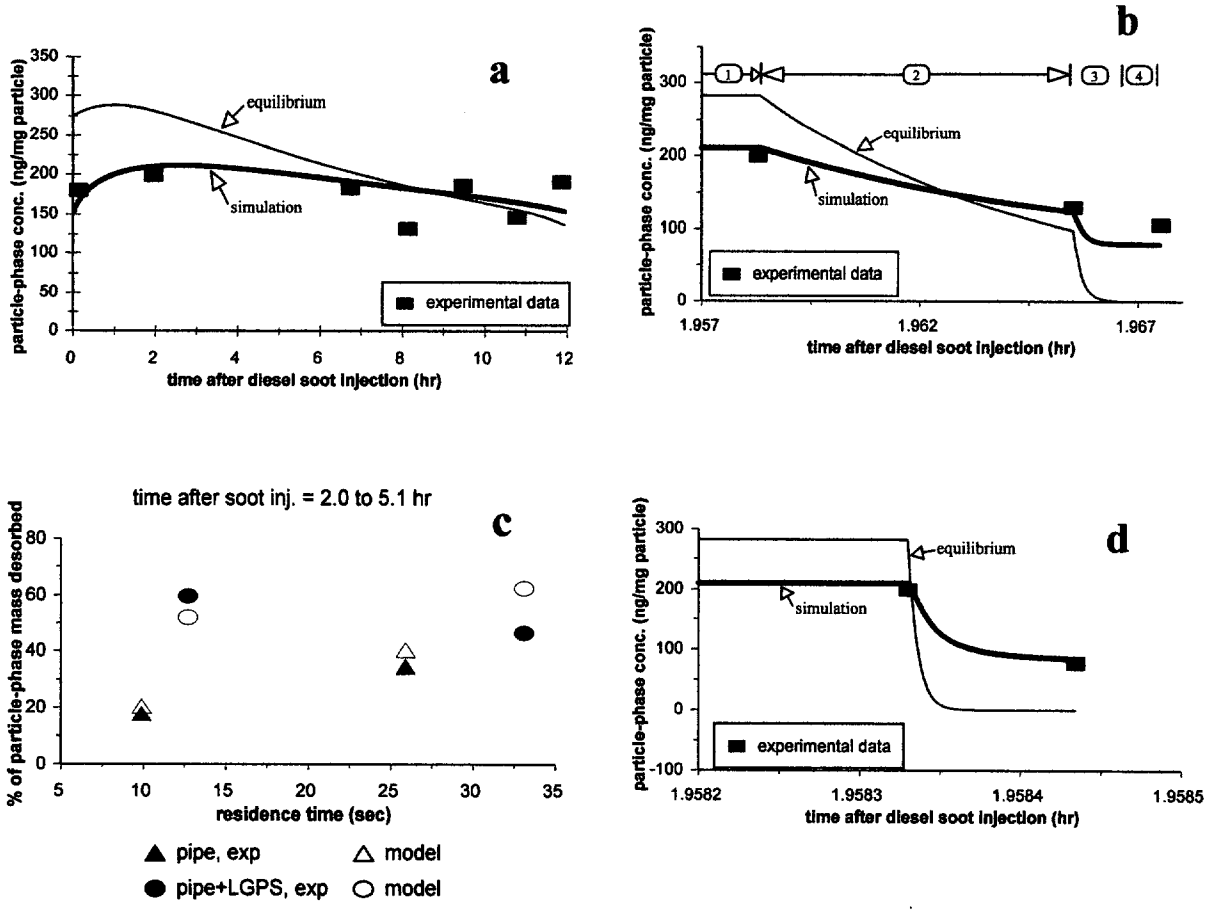

FIGURE A3-1. Select experimental vs simulation results for fluorene-d_{10} using a dual-impedance model. $D_{a,1} = 2.4\text{x}10^{-12}$ cm^2/sec, $D_{a,2} = 4\text{x}10^{-16}$ cm^2/sec. (a) Chamber data. (b) LGPS data. Desorption from particles in: 1. chamber, 2. transfer pipe (t_r=25.9sec), 3. stripping device (t_r=4.1sec), and 4. back of stripping device housing (t_r=3.1sec). (c) Summary of particle desorption results in transfer pipe and stripping device. (d) Desorption from particles in sampling denuder (t_r=0.38sec).

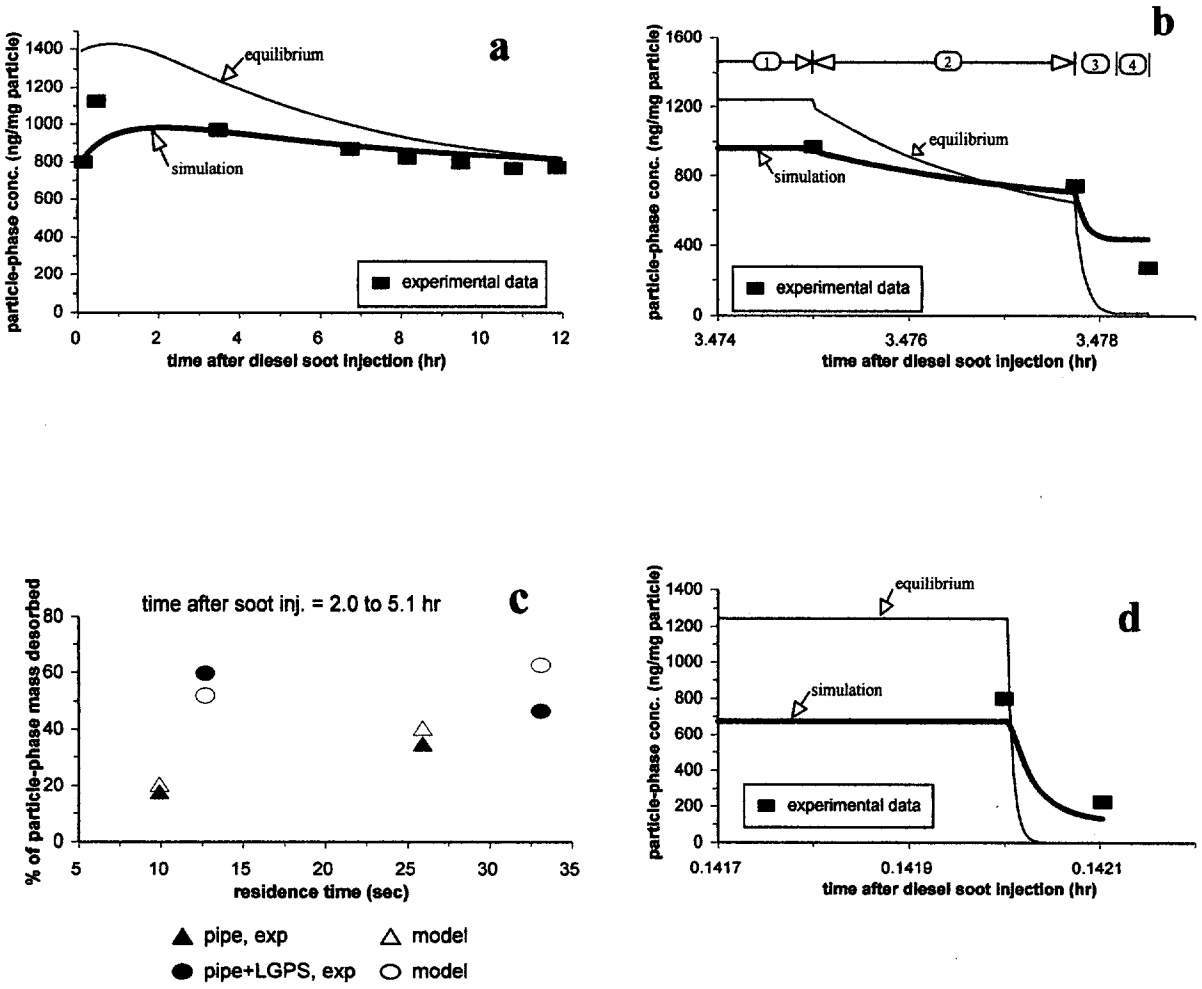

FIGURE A3-2. Select experimental vs simulation results for phenanthrene-d_{10} using a dual-impedance model. $D_{a,1}$ = 6.0x10^{-12} cm^2/sec, $D_{a,2}$ = 3x10^{-16} cm^2/sec. (a) Chamber data. (b) LGPS data. Desorption from particles in: 1. chamber, 2. transfer pipe (t_r=9.9sec), 3. stripping device (t_r=1.6sec), and 4. back of stripping device housing (t_r=1.2sec). (c) Summary of particle desorption results in transfer pipe and stripping device. (d) Desorption from particles in sampling denuder (t_r=0.37sec).

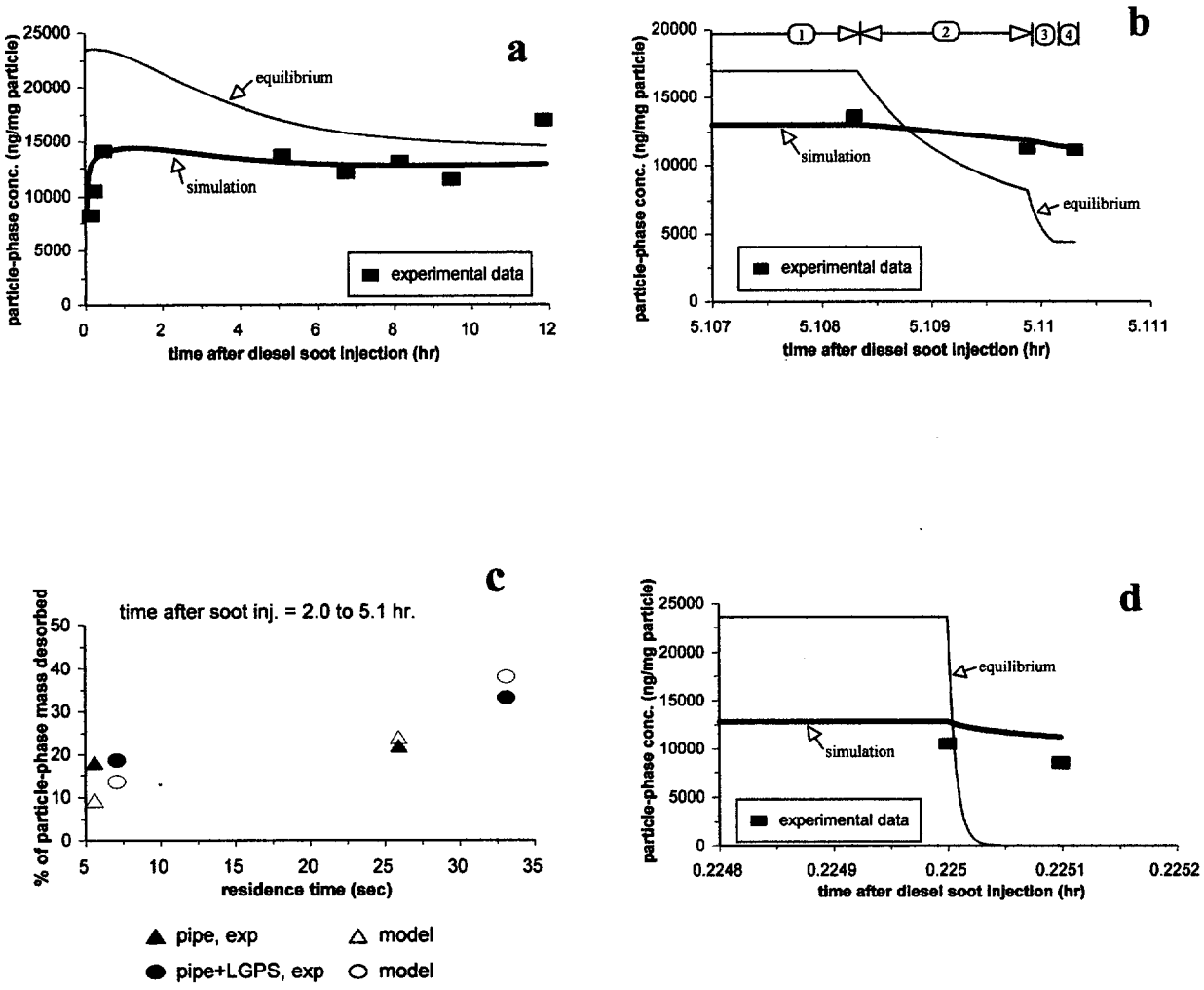

FIGURE A3-3. Select experimental vs simulation results for benz(a)anthracene-d_{12} using a dual-impedance model. $D_{a,1} = 1.8\text{x}10^{-14}$ cm^2/sec, $D_{a,2} = 2\text{x}10^{-16}$ cm^2/sec. (a) Chamber data. (b) LGPS data. Desorption from particles in: 1. chamber, 2. transfer pipe (t_r=5.6sec), 3. stripping device (t_r=0.88sec), and 4. back of stripping device housing (t_r=0.67sec). (c) Summary of particle desorption results in transfer pipe and stripping device. (d) Desorption from particles in sampling denuder (t_r=0.36sec).

APPENDIX 4. Calculation of Gas-Phase PAH Concentration as the Aerosol Passes Through the Transfer Pipe, LGPS, and Sampling Denuders

The theoretical collection efficiency of an annular denuder is given by (*50*)

$$f = 1 - B\exp\left[-\beta\frac{\pi D_g L (d_o + d_i)}{2Q(d_o - d_i)}\right] \quad \text{(A4-1)}$$

where B is a function of the channel geometry ($B = 0.91$ theoretically), β is a function of the wall sticking efficiency (for 100% efficiency, $\beta = 15.01$), D_g is the gas-phase diffusion coefficient of the analyte of interest, L is the length of the denuder parallel to flow, d_o and d_i are the outer and inner diameters of the annulus, respectively, and Q is the volumetric flow rate.

For a parallel plate denuder the equation takes the form (*50*)

$$f = 1 - B\exp\left[-\beta\frac{D_g L (2a + b)^2}{4Qab}\right] \quad \text{(A4-2)}$$

where $B = 0.91$ theoretically, $\beta = 15.08$ for 100% sticking efficiency, b is the long dimension of the denuder cross section, and a is half of the short dimension of the denuder cross section. Gas-phase diffusion coefficients used in eqs A4-1 and A4-2 were calculated using the method of Fuller *et al.* (*51*) which is based on the molar mass and volume of the analyte and the average molar mass and volume of air. Since the geometry of the transfer pipe and the carbon-paper

stripper units in the LGPS did not change in this study, B was set at 0.91. β was obtained for each compound and each sample by optimization using the measured gas-phase PAH concentrations in the chamber vs upstream of the LGPS (to obtain β for the transfer pipe) and upstream vs downstream of the LGPS (to obtain β for the stripper units). Put simply, the value of β was varied until the calculated concentration using eqs A4-1 and A4-2 was equal to the measured concentration exiting the transfer pipe and LGPS, respectively. The gas-phase concentration in the void space behind the stripper units was assumed to remain constant.

Sampling denuder efficiency tests showed that the sampling denuders were >99% efficient. Accordingly, theoretical B and β values were used in eq A4-1 to determine the gas-phase concentration profile in the sampling denuders.

APPENDIX 5. Calculation of K_D

The model of Jang *et al.* (*40*, *41*) can be used to calculate the activity coefficient, γ, of analytes in the organic material of various types of atmospheric particulate matter as a function of temperature and relative humidity using functional group contribution methods. Since this model determines amount of water sorbed by the particle organic material as a function of relative humidity, it can also be used to calculate the average molecular weight of the particle organic material, MW_{om} (g/mol). Using these values, the equilibrium gas-particle partition coefficient, K_p (m^3/mg particle), can be calculated using the following expression (*52*):

$$K_p = \frac{760 f_{om} RT}{10^3 MW_{om} \gamma p_L^o} \qquad \text{(A5-1)}$$

where f_{om} is the mass fraction of organic material in the particles, R is the gas constant (8.2×10^{-5} m^3 atm/mol K), T (K) is the temperature, and p_L^o (Torr) is the pure compound liquid vapor pressure (sub-cooled if necessary) of the analyte of interest at T. Note that eq A5-1 only describes *absorptive* partitioning (i.e., partitioning between the gas and liquid phases).

Comparing the K_p values for fluoranthene-d_{10} in diesel soot obtained using eq A5-1 vs the K_p values obtained from experimental data for a given temperature and relative humidity reveals that the experimental K_p values are significantly higher. Since eq A5-1 only describes absorptive partitioning, whereas the experimental K_p data includes all sources of analyte uptake by particles, it appears that the particles contain additional sorptive capacity above liquid absorption. Since diesel soot particles contain from 20 to 85% nonextractable, carbonaceous

material, adsorption of analytes to this solid material is likely. Thus, rather than simply quantifying the partitioning of an analyte between the air and the particles as:

$$C_p\left(\frac{\text{ng in particles}}{\text{mg particles}}\right) \leftrightarrow C_g\left(\frac{\text{ng in air}}{\text{m}^3\text{ air}}\right) \qquad \text{(A5-2)}$$

where $K_p = C_p / C_g$, partitioning may be quantified between: (a) the air and absorption in the particles' organic material and (b) the organic material and adsorption on the solid portion of the particles as:

$$C_s\left(\frac{\text{ng on solid material}}{\text{mg solid material}}\right) \leftrightarrow C_{om}\left(\frac{\text{ng in om}}{\text{mg om}}\right) \leftrightarrow C_g\left(\frac{\text{ng in air}}{\text{m}^3\text{ air}}\right) \qquad \text{(A5-3)}$$

where $K_D = C_s / C_{om}$ (assuming a linear isotherm), and $K_{p,om}$ is K_p normalized for organic material mass, rather than total particle mass:

$$K_{p,om} = \frac{C_{om}}{C_g} = \frac{K_p}{f_{om}} \qquad \text{(A5-4)}$$

Using the relationships in eqs A5-2 through A5-4, an expression can be derived for the adsorption distribution coefficient, K_D:

$$K_D\left(\frac{\text{mg om}}{\text{mg solid material}}\right) = \frac{C_s}{C_{om}} = \frac{\left(\frac{K_p}{K_{p,om}\, f_{om}} - 1\right)}{\left(\frac{1}{f_{om}} - 1\right)} \qquad \text{(A5-5)}$$

Thus, using the Jang *et al.* group contribution model (*40*, *41*), the values of γ and MW_{om} can be determined as a function of temperature and relative humidity. The subcooled liquid vapor pressure, $p_L°$, may be determined as a function of temperature using the data of Yamasaki (*47*) and the method of Hamilton (*48*, *49*), which is based on the relationship between vapor pressure and relative gas chromatographic retention times. Thus, for a given set of experimental T, f_{om}, and K_p values, the adsorption distribution coefficient, K_D, can be calculated using eqs A5-1, A5-4, and A5-5.

The example in the "sources of microtransport impedances" section of the text involves the partitioning of fluoranthene-d_{10} at a time of 3 hrs after diesel soot injection in the present study. At that time, the chamber temperature is 285 K, and the relative humidity is 70%. Applying the UNIFAC-based model of Jang *et al.* (*40*, *41*) results in an activity coefficient, γ, of 4.4 and an average molecular weight of the organic material, MW_{om}, of 238 g/mol. This calculation uses the diesel soot organic material composition reported in Jang *et al.* (*40*, *41*), which is based on the characterization work of Rogge *et al.* (*31*). The experimental f_{om} is 0.37, and the calculated fluoranthene-d_{10} $p_L°$ is 1.0×10^{-5} Torr. The K_p value, obtained from the semi-empirical expression shown in eq A2-1 (see Appendix 2 of Supporting Information), is 1.2 mg

particle/m^3. Substitution into eqs A5-1, A5-4, and A5-5 yields a K_D value of 0.6 mL om/g solid material.

APPENDIX 6. Calculation of the Differences in Free-Liquid Diffusion Coefficients, D_l, Between PAHs

The free-liquid diffusion coefficient may be estimated using the Wilke-Chang equation (*53*):

$$D_l = 7.4 \times 10^{-8} (\phi_S^\circ MW_{om})^{0.5} \frac{T}{\mu_v V_{mo}^{0.6}} \qquad \text{(A6-1)}$$

where ϕ_S° is a solvent (i.e., organic material) association term, MW_{om} (g/mol) is the molecular weight of the solvent, T (K) is the temperature, μ_v (cP) is the solvent viscosity, and V_{mo} (cm^3/mol) is the molecular volume of the analyte. Since V_{mo}, is the only parameter in eq A6-1 that is dependent on the analyte of interest (the remaining variables are dependent on the solvent), the relative magnitude of D_l values for a series of compounds can be calculated from the compounds' molecular volumes:

TABLE A6-1. Molecular Volume Increments

atom or feature in molecule	volume increment (cm^3/mol)
carbon	14.8
hydrogen	3.7
five-membered ring	-11.5
six-membered ring	-15.0

Source: Perry and Chilton (*54*)

$$\frac{D_{l,cmpd1}}{D_{l,cmpd2}} = \left(\frac{V_{mo,cmpd2}}{V_{mo,cmpd1}} \right)^{0.6} \qquad \text{(A6-2)}$$

Molecular volumes can be estimated by adding the atomic volumes for the elements in the molecule and adjusting for specific molecular features, such as rings. The volume increments of interest for PAHs are given in Table A6-1, and the calculated D_l values relative to benz(a)anthracene are shown in Table A6-2. Note that these calculations are for the hydrogenated PAHs rather than the deuterated PAHs. The values for the deuterated PAHs will not be significantly different, since the additional neutron in the hydrogen atoms will not change the atomic volume significantly.

TABLE A6-2. Calculated Molecular Volumes and Free-Liquid Diffusion Coefficients Relative to Benz(a)anthracene

PAH	molecular volume (cm^3/mol)	$D_{l,PAH} / D_{l,BaA}$
fluorene	188.2	1.19
phenanthrene	199.2	1.15
fluoranthene	217.3	1.09
benz(a)anthracene	250.8	1.00